PROCEEDINGS OF SCIENCE

Quantum-correlated $D\bar{D}$ inputs to CKM angle γ from BESIII

Lei Li[*†]
Beijing Institute of Petrochemical Technology & University of Oxford
E-mail: lilei2014@bipt.edu.cn

Measurements are presented of the relative strong-phase parameters between D^0 and $\bar{D}^0$ in the decays $D^0 \to K_{S,L}\pi^+\pi^-$ are using 2.93 fb^{-1} of data collected at $\sqrt{s}$=3.773 GeV by the BESIII detector. The results can provide the key inputs in model independent measurments of CKM angle γ. Using these parameters, the associated uncertainty on the Cabibbo-Kobayashi-Maskawa angle γ/ϕ_3 is expected to be approximately a factor of three smaller than that from previous measurements by the CLEO collaboration, for an analysis using the decay $B^\pm \to DK^\pm$, $D \to K^0_S\pi^+\pi^-$, where D represents a superposition of D^0 and $\bar{D}^0$ states.

18th International Conference on B-Physics at Frontier Machines - Beauty2019 -
29 September / 4 October, 2019
Ljubljana, Slovenia

[*]Speaker.
[†]On behalf of the BESIII Collaboration.

PoS(Beauty2019)006

1. Introduction

The study of quantum-correlated charm-meson pairs produced at threshold allows unique access to hadronic decay properties that are of great interest across a wide range of physics applications. In particular, determination of the strong-phase parameters provides vital input to measurements of the Cabibbo-Kobayashi-Maskawa (CKM) [1] angle γ (also denoted ϕ_3) and other *CP*-violating observables. The unitarity triangle angle γ is of particular interest since it is the only one that can easily be extracted in tree-level processes, in which the contribution of non-SM effects is expected to be very small [2]. Therefore, a measurment of γ provides a benchmark of the SM with negligible theoretical uncertainties. A precision measurement of γ is an essential ingredient in testing the SM description of *CP*-violation and can probe for new physics via the comparison of direct and indirect measurements [3].

One of the most sensitive decay channels for measuring γ is $B^- \to DK^-$, $D \to K^0_S\pi^+\pi^-$ [4] where D represents a superposition of D^0 and $\bar{D}^0$ mesons. The amplitude of the B^- decay can be written as

$$f_{B^-}(m^2_+, m^2_-) \propto f_D(m^2_+, m^2_-) + r_B e^{i(\delta_B - \gamma)} f_{\bar{D}}(m^2_+, m^2_-). \tag{1.1}$$

Here, m^2_+ and m^2_- are the squared invariant masses of the $K^0_S\pi^+$ and $K^0_S\pi^-$ pairs from the $D^0 \to K^0_S\pi^+\pi^-$ decay, $f_D(m^2_+, m^2_-)(f_{\bar{D}}(m^2_+, m^2_-))$ is the amplitude of the $D^0(\bar{D}^0)$ decay to $K^0_S\pi^+\pi^-$ at (m^2_+, m^2_-) in the Dalitz plot, r_B is the ratio of the suppressed amplitude to the favored amplitude, and δ_B is the *CP*-conserving strong-phase difference between them. If the small second-order effects of charm mixing and *CP* violation [4, 5, 6, 7, 8] are ignored, Eq. (1.1) can be written as

$$f_{B^-}(m^2_+, m^2_-) \propto f_D(m^2_+, m^2_-) + r_B e^{i(\delta_B - \gamma)} f_D(m^2_-, m^2_+) \tag{1.2}$$

through the use of the relation $f_{\bar{D}}(m^2_+, m^2_-) = f_D(m^2_-, m^2_+)$. The square of the amplitude clearly depends on the strong-phase difference $\Delta\delta_D \equiv \delta_D(m^2_+, m^2_-) - \delta_D(m^2_-, m^2_+)$, where $\delta_D(m^2_+, m^2_-)$ is the strong phase of $f_D(m^2_+, m^2_-)$. While the strong-phase difference can be inferred from an amplitude model of the decay $D^0 \to K^0_S\pi^+\pi^-$, such an approach introduces model-dependence in the measurement. This property is undesirable as the systematic uncertainty associated with the model is difficult to estimate reliably, since common approaches to amplitude-model building break the optical theorem [9]. Instead, the strong-phase differences may be measured directly in the decays of quantum-correlated neutral D meson pairs created in the decay of the $\psi(3770)$ resonance [4, 7]. This approach ensures a model-independent [10, 11, 12, 13, 14] measurement of γ where the uncertainty in the strong-phase knowledge can be reliably propagated.

The strong-phase differences in $D \to K^0_S\pi^+\pi^-$ were first studied in this manner by the CLEO collaboration using 0.82 fb^{-1} of data [15, 16]. These measurements are limited by their statistical precision, and this precision is insufficient to avoid leading uncertainty contributions to the measurements of γ and mixing and *CP*-violation in the charm sector anticipated in the near future. The BESIII detector at the BEPCII collider has the largest data sample collected at the $\psi(3770)$ resonance, corresponding to an integrated luminosity of 2.93 fb^{-1}. Therefore with the BESIII data it is possible to substantially improve the knowledge of the strong-phase differences, which will reduce the associated uncertainty when used in other *CP*-violation measurements.

2. Formalism

The analysis of the data is performed in regions of phase space. Measurements are presented in three schemes which are identical to those used in Ref. [16]. All schemes divide the phase space into eight pairs of bins, symmetrically along the $m_+^2 = m_-^2$ line. The bins are indexed with i, running from -8 to 8 excluding zero. The bins have a positive index if their position satisfies $m_+^2 < m_-^2$, and the exchange of coordinates $(m_+^2, m_-^2) \leftrightarrow (m_-^2, m_+^2)$, changes the sign of the bin. The choice of division of the phase space has an impact on the sensitivity of the *CP*-violation measurements that use this strong-phase information as input. The schemes are irregular in shape and are shown in Fig. 1. Detailed information on the choice of these regions is given in Ref. [16]. The scheme denoted "equal $\Delta\delta_D$ binning" defines regions such that the variation in $\Delta\delta_D$ over each bin is minimized, and is based on a model developed on flavor-tagged data [17] to partition the phase space. In the half of the Dalitz plot $m_+^2 < m_-^2$, the i^{th} bin is defined by the condition

$$2\pi(i-3/2)/8 < \Delta\delta_D(m_+^2, m_-^2) < 2\pi(i-1/2)/8. \tag{2.1}$$

A more sensitive binning scheme for the measurement of γ is denoted the "optimal binning". This binning takes into account both the model of the $D^0 \to K_S^0\pi^+\pi^-$ decay and the expected distribution of D decays arising from the process $B^- \to DK^-$ when determining the bins. This choice improves the sensitivity of γ measurements compared to the equal binning by approximately 10%. The third binning scheme, denoted the "modified optimal binning" is useful in analysing samples with low yields [12]. Although these three binning schemes are based on the $D^0 \to K_S^0\pi^+\pi^-$ model reported in Ref. [17], this procedure does not introduce model-dependence into the analyses that employ the resulting strong-phase measurements.

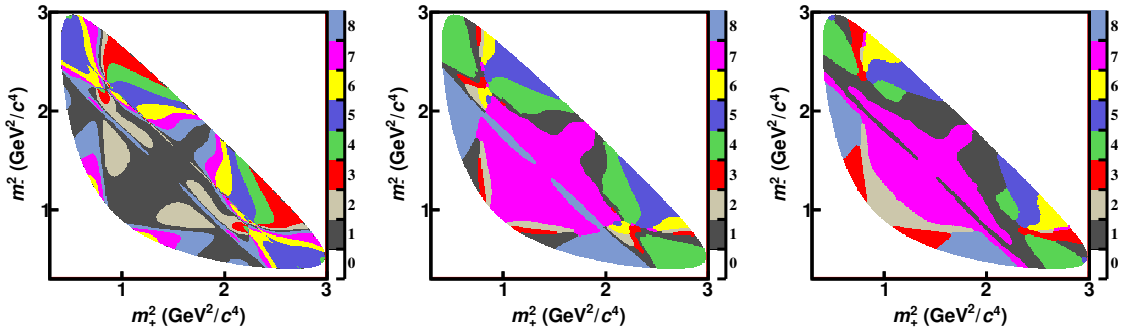

Figure 1: The (left) equal $\Delta\delta_D$, (middle) optimal and (right) modified optimal binnings of the $D \to K_{S,L}^0\pi^+\pi^-$ Dalitz plot [16]. The color scale represents the absolute value of the bin number $|i|$.

The interference between the amplitudes of the D^0 and $\bar{D}^0$ decays can be parameterized by two quantities c_i and s_i, which are the amplitude-weighted averages of $\cos\Delta\delta_D$ and $\sin\Delta\delta_D$ over each Dalitz plot bin. They are defined as

$$c_i = \frac{1}{\sqrt{F_i F_{-i}}} \int_i |f_D(m_+^2, m_-^2)||f_D(m_-^2, m_+^2)| \times \cos[\Delta\delta_D(m_+^2, m_-^2)] dm_+^2 dm_-^2, \tag{2.2}$$

and

$$s_i = \frac{1}{\sqrt{F_i F_{-i}}} \int_i |f_D(m_+^2, m_-^2)||f_D(m_-^2, m_+^2)| \times \sin[\Delta\delta_D(m_+^2, m_-^2)] dm_+^2 dm_-^2, \tag{2.3}$$

where F_i is the fraction of events found in the i^{th} bin of the flavor-specific decay $D^0 \to K_S^0\pi^+\pi^-$.

The $\psi(3770)$ has a $C = -1$ quantum number and this is conserved in the strong decay, which produces two neutral D mesons. Hence the two neutral D mesons have an anti-symmetric wave-function. This also means that the two D mesons do not decay independently of one another.

In the case where one D meson decays to a CP-even eigenstate, the properties of the anti-symmetric wave-function mean that the other D meson decays to a CP-odd final state. Considering a pair of decays where one D meson decays to CP eigenstate, referred to as "the tag", and the other D meson decays to the $K_S^0\pi^+\pi^-$ final state, the decay amplitude of the $D \to K_S^0\pi^+\pi^-$ decay is given by

$$f_{CP\pm}(m_+^2, m_-^2) = \frac{1}{\sqrt{2}}[f_D(m_+^2, m_-^2) \pm f_D(m_-^2, m_+^2)], \tag{2.4}$$

where $f_{CP^\pm}$ refers to the CP eigenvalue of the $D \to K_S^0\pi^+\pi^-$ decay. It is possible to generalize this expression to include decays where the tag D meson decays to a self-conjugate final state rather than a CP eigenstate, assuming that the CP-even fraction, F_{CP}, is known. The number of events, M_i, observed in the i^{th} bin, where the tag D meson decays to a self-conjugate final state is then given by

$$M_i = h_{CP}(K_i - (2F_{CP} - 1)2c_i\sqrt{K_i K_{-i}} + K_{-i}), \tag{2.5}$$

where h_{CP} is a normalization factor. The value of F_{CP} is 1 for CP-even tags and 0 for CP-odd tags. This parameterization is valuable since it allows for final states with very high or very low CP-even fractions to be used to provide sensitivity to the c_i parameters. A good example of such a decay is the mode $D \to \pi^+\pi^-\pi^0$ where the fractional CP-even content is measured to be $F_{CP}^{\pi\pi\pi^0} = 0.973 \pm 0.017$ [18].

However, from Eq. (2.2), the sign of $\Delta\delta_D$ is undetermined if only the values of c_i are known from the CP-tagged $D \to K_S^0\pi^+\pi^-$ decay. Important additional information can be gained to determine the s_i parameters by studying the Dalitz-plot distributions where both D mesons decay to $K_S^0\pi^+\pi^-$. The amplitude of the $\psi(3770)$ decay is in this case given by

$$f(m_+^2, m_-^2, m_+^{2\dagger}, m_-^{2\dagger}) = \frac{f_D(m_+^2, m_-^2) f_D(m_-^{2\dagger}, m_+^{2\dagger}) - f_D(m_+^{2\dagger}, m_-^{2\dagger}) f_D(m_-^2, m_+^2)}{\sqrt{2}}, \tag{2.6}$$

where the use of the $'\dagger'$ symbol differentiates the Dalitz plot coordinates of the two $D \to K_S^0\pi^+\pi^-$ decays. The observable M_{ij} is defined as the event yield in the i^{th} bin of the first and the j^{th} bin of the second $D \to K_S^0\pi^+\pi^-$ Dalitz plot, and is given by

$$M_{ij} = h_{\text{corr}}[K_i K_{-j} + K_{-i} K_j - 2\sqrt{K_i K_{-j} K_{-i} K_j}(c_i c_j + s_i s_j)], \tag{2.7}$$

where h_{corr} is a normalization factor. Equation (2.7) is not sensitive to the sign of s_i, however, this ambiguity can be resolved using a weak model assumption.

In order to improve the precision of the c_i and s_i parameters it is useful to increase the possible tags to include $D \to K_L^0\pi^+\pi^-$ which is closely related to the $D \to K_S^0\pi^+\pi^-$ decay. The convention

Table 1: A list of tag decay modes used in the measurement.

Tag group	
Flavor	$K^+\pi^-$, $K^+\pi^-\pi^0$, $K^+\pi^-\pi^-\pi^+$, $K^+e^-\bar{\nu}_e$
CP-even	K^+K^-, $\pi^+\pi^-$, $K^0_S\pi^0\pi^0$, $K^0_L\pi^0$, $\pi^+\pi^-\pi^0$
CP-odd	$K^0_S\pi^0$, $K^0_S\eta$, $K^0_S\omega$, $K^0_S\eta'$, $K^0_L\pi^0\pi^0$
Mixed-*CP*	$K^0_S\pi^+\pi^-$

$A(D^0 \to K^0_S\pi^+\pi^-) = A(\bar{D}^0 \to K^0_S\pi^-\pi^+)$ is used. Then, since the K^0_S and K^0_L mesons are, to an excellent approximation, of opposite *CP*, it follows that $A(D^0 \to K^0_L\pi^+\pi^-) = -A(\bar{D}^0 \to K^0_L\pi^-\pi^+)$. Hence, where $D \to K^0_L\pi^+\pi^-$ is used as the signal decay, and the tag is a self-conjugate final state, the event yield M'_i is given by

$$M'_i = h_{CP}(K'_i + (2F_{CP}-1)2c_i\sqrt{K'_iK'_{-i}} + K'_{-i}), \tag{2.8}$$

where K'_i and c'_i are associated to the $D \to K^0_L\pi^+\pi^-$ decay. The event yield M'_{ij}, corresponding to the yield of events where the $D \to K^0_S\pi^+\pi^-$ decay is observed in the i^{th} bin and the $D \to K^0_L\pi^+\pi^-$ decay is observed in the j^{th} bin is given by

$$M'_{ij} = h_{\text{corr}}[K_iK'_{-j} + K_{-i}K'_j + 2\sqrt{K_iK'_{-j}K_{-i}K'_j}(c_ic'_j + s_is'_j)], \tag{2.9}$$

where s'_i is the amplitude-weighted average sine of the strong-phase difference for the $D \to K^0_L\pi^+\pi^-$ decay.

The normalization factors h_{CP} and h_{corr} can be related to the yields of reconstructed signal and tag final states and the number of neutral D meson pairs $N_{D\bar{D}}$ produced in the data set, with $h_{CP} \propto S_{CP}/S_{\text{FT}}$ and $h_{\text{corr}} \propto N_{D\bar{D}}/(S^2_{\text{FT}})$. Here S_{CP} is the yield of *CP*-tagged signal decays, and S_{FT} refers to the combined yields of flavor-tagged signal decays.

3. Analysis

In order to measure c_i, s_i, c'_i and s'_i, a range of single-tag (ST) and double-tag (DT) samples of D decays are reconstructed. The ST samples are those where the decay products of only one D meson are reconstructed. The DT samples are those where one D meson decays to the signal mode $K^0_S\pi^+\pi^-$ or $K^0_L\pi^+\pi^-$ and the other D meson decays to one of the tag modes listed in Table 1. Tag decay modes fall into the categories of flavor, *CP* eigenstates or mixed-*CP*. Flavor tags identify the flavor of the decaying meson through a semi-leptonic decay or a Cabibbo-favored hadronic decay. *CP* eigenstates and mixed-*CP* tags identify a decay from an initial state which is a superposition of D^0 and $\bar{D}^0$. The $D \to \pi^+\pi^-\pi^0$ tag is used for the first time to measure the strong-phase parameters in $D \to K^0_{S,L}\pi^+\pi^-$ decays. It has a relatively high BF and selection efficiency resulting in a large increase to the *CP*-tagged yields. The use of this tag is possible through the knowledge of F_{CP} for this decay [18]. In this paper the $D \to \pi^+\pi^-\pi^0$ is referred to as a *CP*-even eigenstate, although its small *CP*-odd component is always taken into account, as in Eq. (2.5).

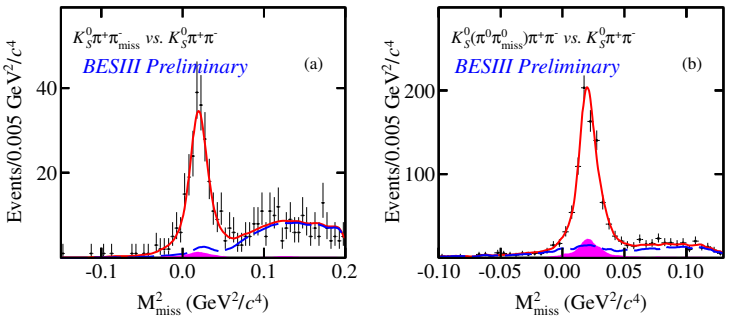

Figure 2: Fits to $M^2_{\rm miss}$ distributions in data. Points with error bars are data, long-dashed (blue) curves are the fitted combinatorial backgrounds. The shaded areas (pink) show MC estimates of the peaking backgrounds from (a) $D \to \pi^+\pi^-\pi^+\pi^-$ and (b) $D \to \pi^+\pi^-\pi^0\pi^0$, and the red solid curves are the total fits.

The DT yield of $K^0_S\pi^+\pi^-$ *vs.* $K^0_S\pi^+\pi^-$ is crucial for extracting the s_i values and thus it is desirable to increase the reconstruction efficiency for these events. Therefore three independent selections are introduced in order to maximize the yield of $D \to K^0_S\pi^+\pi^-$ *vs.* $D \to K^0_S\pi^+\pi^-$ candidates. The first selection requires that both $K^0_S\pi^+\pi^-$ final states on the signal and tag side are fully reconstructed. The second selection class allows for one pion originating from the D meson to be unreconstructed, denoted as $K^0_S\pi^+\pi^-_{\rm miss}$. Events with only three remaining charged tracks recoiling against the $D \to K^0_S\pi^+\pi^-$ ST are searched for. The missing pion is inferred by calculating the missing-mass squared ($M^2_{\rm miss}$) of the event, which is defined as

$$M^2_{\rm miss} = (\sqrt{s}/2 - \sum_i E_i)^2 - |\vec{p}_{\rm sig} - \sum_i \vec{p}_i|^2, \tag{3.1}$$

where $\vec{p}_{\rm sig}$ is the momentum of the fully reconstructed $D \to K^0_S\pi^+\pi^-$ candidate and $\sum_i E_i$ and $\sum_i \vec{p}_i$ are the sum of the energy and momentum of the other reconstructed particles that form the partially reconstructed D meson candidate. Figure 2 (a) shows the $M^2_{\rm miss}$ distribution from the partially reconstructed $D \to K^0_S\pi^+\pi^-$ *vs.* $D \to K^0_S\pi^+\pi^-_{\rm miss}$ candidates. The distribution peaks at $M^2_{\rm miss} \sim 0.02$ GeV$^2/c^4$, which is consistent with the missing particle being a $\pi^\pm$. The peaking backgrounds are approximately 3% of the signal yield and are primarily from the $D \to \pi^+\pi^-\pi^+\pi^-$ decay. The third $D \to K^0_S\pi^+\pi^-$ *vs.* $D \to K^0_S\pi^+\pi^-$ selection identifies those events where one K^0_S meson decays to a $\pi^0\pi^0$ pair. Events where there are only two remaining oppositely-charged tracks recoiling against the ST $D \to K^0_S\pi^+\pi^-$ are selected and these tracks are classified as the π^+ and π^- from the D meson. To avoid the reduced efficiency associated with reconstructing both π^0 mesons from the K^0_S, only one of the them is searched for. This type of tag is referred to as $K^0_S(\pi^0\pi^0_{\rm miss})\pi^+\pi^-$. The missing-mass squared of the event is defined in the same way as in Eq. (3.1) and the summation is over the π^+, π^-, and π^0 mesons that are reconstructed on the tag side. A further variable, $M'^2_{\rm miss}$, where the reconstructed π^0 is also not included in the summed energies and momenta of the tag-side particles is also computed. For true $D \to K^0_S\pi^+\pi^-$ decays this variable should be consistent with the square of the K^0_S meson nominal mass. Therefore, candidates that do not satisfy $0.22 < M'^2_{\rm miss} < 0.27$ GeV$^2/c^4$ are removed from the analysis in order to suppress background from $D \to \pi^+\pi^-\pi^0\pi^0$ decays. Figure 2 (b) shows the resultant $M^2_{\rm miss}$ distribution of the accepted candidates in data. There remains a contribution of peaking background dominated

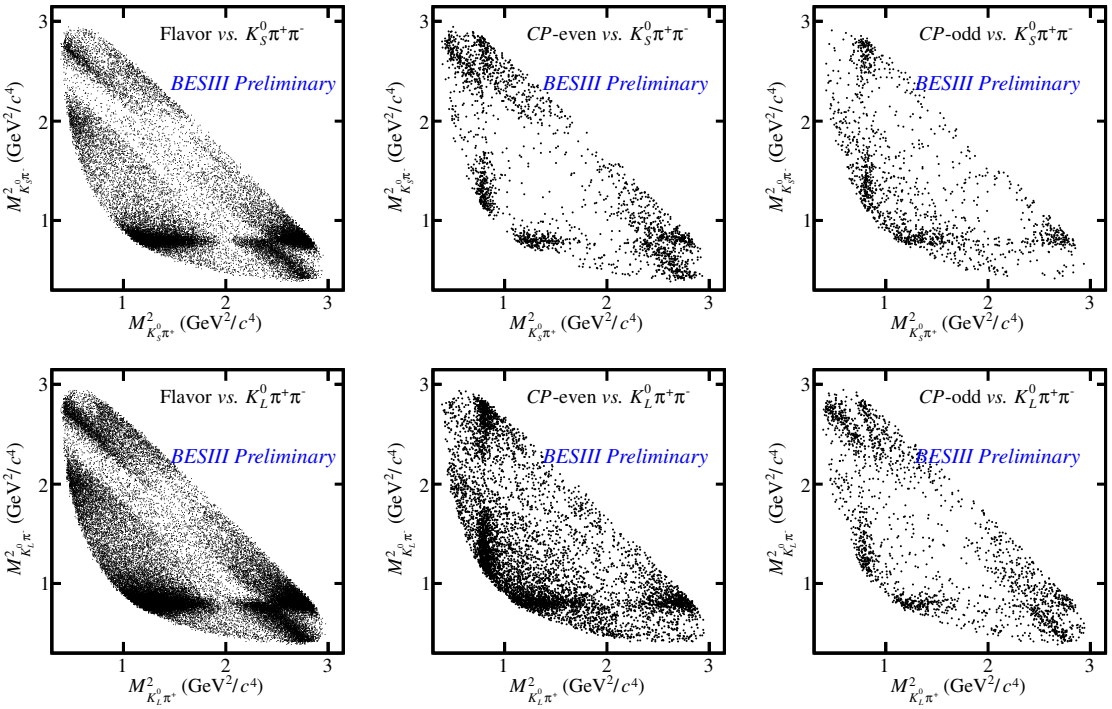

Figure 3: Dalitz plots of $K^0_S\pi^+\pi^-$ and $K^0_L\pi^+\pi^-$ events in data.

from $D \to \pi^+\pi^-\pi^0\pi^0$ decays, where the rate relative to signal is determined from simulated data to be around 15%.

Overall, the DT yields of $D \to K^0_{S(L)}\pi^+\pi^-$ involving a *CP* eigenstate are a factor of 5.3 (9.2) larger than those in Ref. [16], and the DT yields of $K^0_S\pi^+\pi^-$ tagged with $D \to K^0_{S(L)}\pi^+\pi^-$ decays are a factor of 3.9 (3.0) larger than those in Ref. [16]. These increases come not only from the larger dataset available at BESIII but also from the additional tag modes and the application of partial-reconstruction techniques for $D \to K^0_S\pi^+\pi^-$. The Dalitz plots for $D^0 \to K^0_S\pi^+\pi^-$ and $D^0 \to K^0_L\pi^+\pi^-$ *vs.* the flavor tags selected from the data are shown in Fig. 3. In order to merge the D^0 and $\bar{D}^0$ decays the exchange of coordinates $M^2_{K^0_{S,L}\pi^\pm} \leftrightarrow M^2_{K^0_{S,L}\pi^\mp}$ is performed for the $\bar{D}^0$ decays. Figure 3 also shows the *CP*-even and *CP*-odd tagged signal channels selected in the data. The effect of the quantum correlation in the data is immediately obvious by studying the differences in these plots. Most noticeably, the *CP*-odd component $D \to K^0_S\rho^0$ is visible in the $D \to K^0_S\pi^+\pi^-$ decay when tagged by *CP*-even decays, but is absent when tagged by *CP*-odd decays.

It should be noted that detector resolution effects can cause individual events to migrate between Dalitz plot bins after reconstruction. Such migration effects vary among bins due to the irregular bin shapes, coupled with the rapid variations of the Dalitz plot density. Furthermore, migrations differ between $D \to K^0_S\pi^+\pi^-$ and $D \to K^0_L\pi^+\pi^-$ decays due to differing resolutions in the Dalitz plots (0.0068 GeV$^2/c^4$ for $D \to K^0_S\pi^+\pi^-$ and 0.0105 GeV$^2/c^4$ for $D \to K^0_L\pi^+\pi^-$). The resultant bin migrations range within (3-12)% and (3-18)% for the $K^0_S\pi^+\pi^-$ and $K^0_L\pi^+\pi^-$ signals, respectively. Therefore, in the extraction of the expected DT yields, simulated efficiency matrices

are introduced to account for bin migration and reconstruction efficiencies. Studies indicate that neglecting bin migration introduces biases in the determination of c_i (s_i) that average a factor of 0.7 (0.3) times the statistical uncertainty of this analysis, so it is important to correct for this effect.

4. The preliminary strong-phase results at BESIII

The values of $c_i^{(\prime)}$ and $s_i^{(\prime)}$ are obtained by minimizing the negative log-likelihood function constructed as

$$\begin{aligned} -2\log\mathscr{L} = & -2\sum_i\sum_j \log P(N_{ij}^{\rm obs}, \langle N_{ij}^{\rm exp}\rangle)_{K_S^0\pi^+\pi^-, K_{S(L)}^0\pi^+\pi^-} \\ & -2\sum_i \log P(N_i^{\rm obs}, \langle N_i^{\rm exp}\rangle)_{CP, K_{S(L)}^0\pi^+\pi^-} + \chi^2, \end{aligned}$$

where $P(N^{\rm obs}, \langle N^{\rm exp}\rangle)$ is the Possion probability to observe $N^{\rm obs}$ events given the expected number $\langle N^{\rm exp}\rangle$. Here the sums are over the bins of the $D^0 \to K_{S(L)}^0\pi^+\pi^-$ Dalitz plots. The χ^2 penalty term is used to constrain the difference $c_i' - c_i$ ($s_i' - s_i$) to the predicted quantity Δc_i (Δs_i). The values of Δc_i and Δs_i are estimated based on the decay amplitudes of $D^0 \to K_S^0\pi^+\pi^-$ [19] and $D^0 \to K_L^0\pi^+\pi^-$, where the latter is constructed by adjusting the $D^0 \to K_S^0\pi^+\pi^-$ model following the principle that K_S^0 and K_L^0 mesons are of opposite CP, as is discussed in Refs. [15, 16].

The preliminary results of the measured strong-phase parameters $c_i^{(\prime)}$ and $s_i^{(\prime)}$ are presented in Fig. 4. Their systematic uncertainties arise from the evaluation of K_i and K_i', the estimation of ST yields, the MC statistics, subtraction of the DT peaking background, the fitting procedure for extracting DT yields, the difference in momentum resolution between data and MC, and the effects of $D^0\bar{D}^0$ mixing. Study shows that the results of measured strong-phase parameters are limited by their statistical uncertainties. In addition to our results, Fig. 4 includes the predictions of Ref. [19] and the results from Ref. [16], which show reasonable agreement.

The uncertainty on γ due to the measured uncertainties on c_i and s_i is found to be approximately a factor of three smaller than from the CLEO measurements [16]. The predicted statistical uncertainties on γ from LHCb prior to the start of High-Luminosity LHC operation in the mid 2020s, and from Belle II are expected to be 1.5° [20, 21]. Therefore the uncertainty associated to the strong-phase measurements presented here will not be dominant in the determination of γ for Belle II or for LHCb until then.

5. Summary

The preliminary results of the relative strong-phase differences between D^0 and $\bar{D}^0 \to K_{S,L}\pi^+\pi^-$ in bins of phase space are presented. These results are on average a factor 2.5 (1.9) more precise for c_i (s_i) and a factor 2.8 (2.2) more precise for c_i' (s_i') than the previous measurements of these parameters [16]. This improvement arises from the combination of a larger data sample, an increased variety of CP tags, and broader use of the partial reconstruction technique to improve efficiency. This improved precision will ensure that measurements of γ from LHCb and BELLE II over the next decade are not limited by the knowledge of these strong-phase parameters, and also be invaluable in studies of charm mixing and CP-violation.

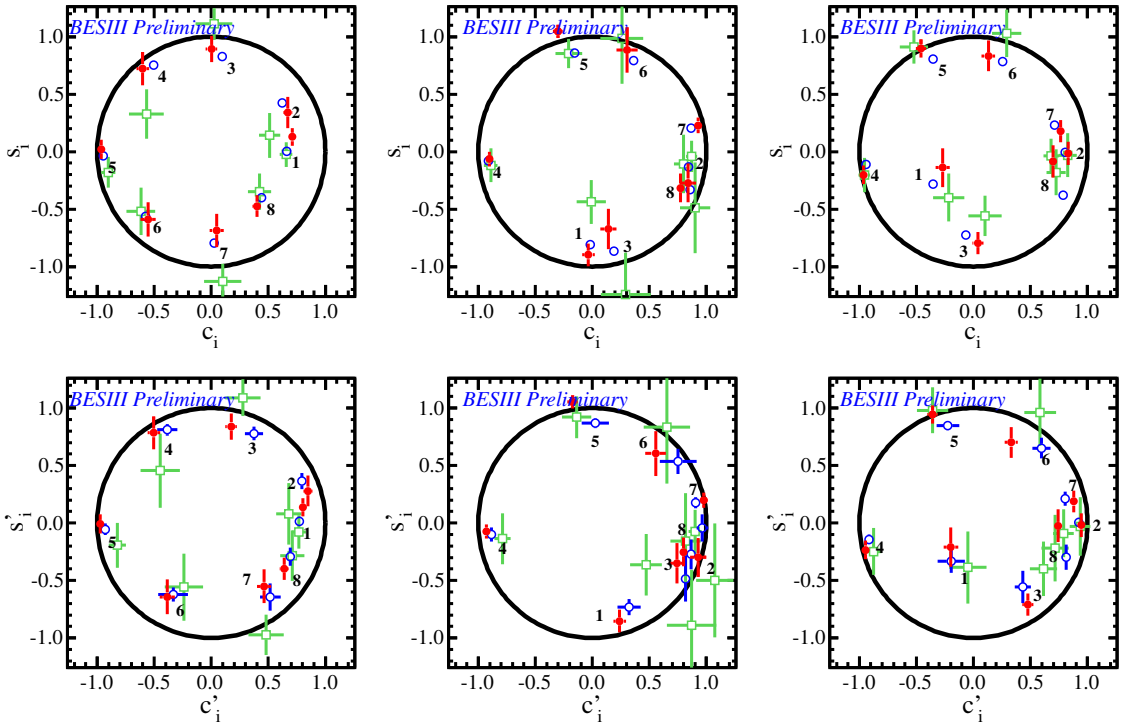

Figure 4: The preliminary results of $c_i^{(\prime)}$ and $s_i^{(\prime)}$ measured in this work (red dots with error bars), the expcted values from Ref. [19] (blue open circles) as well as CLEO results (green open squares with error bars) in Ref. [16]. The top plots are from the equal $\Delta\delta_D$ binning, the middle plots from the optimal binning and plots from the modified optimal binning scheme are on the bottom. The circle indicates the boundary of the physical region $c_i^{(\prime)2} + s_i^{(\prime)2} = 1$.

References

[1] N. Cabibbo, Phys. Rev. Lett. **10**, 531 (1963); M. Kobayashi and T. Maskawa, Prog. Theor. Phys. **49**, 652 (1973).

[2] J. Brod and J. Zupan, J. High Energy Phys. **01** (2014) 051.

[3] M. Blanke and A. Buras, Eur. Phys. J. C **79**, 159 (2019).

[4] A. Giri, Y. Grossman, A. Soffer, and J. Zupan, Phys. Rev. D **68**, 054018 (2003).

[5] Y. Grossman, A. Soffer, and J. Zupan, Phys. Rev. D **72**, 031501(R) (2005).

[6] A. Bondar, A. Poluektov and V. Vorobiev, Phys. Rev. D **82**, 034033 (2010).

[7] A. Bondar and A. Poluektov, Eur. Phys. J. C **47**, 347 (2006); Eur. Phys. J. C **55**, 51 (2008).

[8] A. Bondar, A. Dolgov, A. Poluektov and V. Vorobiev, Eur. Phys. J. C **73**, 2476 (2013).

[9] M. Battaglieri *et al*., Acta Phys. Polon. B **46**, 257 (2015).

[10] R. Aaij *et al*. (LHCb Collaboration), Phys. Lett. B **718**, 43 (2012).

[11] R. Aaij *et al*. (LHCb Collaboration), J. High Energy Phys. **10** (2014) 097.

[12] R. Aaij *et al*. (LHCb Collaboration), J. High Energy Phys. **06** (2016) 131.

[13] R. Aaij *et al*. (LHCb Collaboration), J. High Energy Phys. **08** (2018) 176; Erratum: J. High Energy Phys. **08** (2018) 107.

[14] H. Aihara *et al*. (Belle Collaboration), Phys. Rev. D **85**, 112014 (2012).

[15] R. A. Briere *et al*. (CLEO Collaboration), Phys. Rev. D **80**, 032002 (2009).

[16] J. Libby *et al*. (CLEO Collaboration), Phys. Rev. D **82**, 112006 (2010).

[17] B. Aubert *et al*. (BaBar Collaboration), Phys. Rev. D **78**, 034023 (2008).

[18] M. Nayak *et al*., Phys. Lett. B **747**, 9 (2015).

[19] I. Adachi *et al*. (BaBar and Belle Collaborations), Phys. Rev. D **98**, 110212 (2018).

[20] I. Bediaga *et al*. (LHCb Collaboration), HCB-PUB-2018-009, CERN-LHCC-2018-027 [arXiv:1808.08865].

[21] E. Kou *et al*. (Belle II Collaboration), KEK Preprint 2018-27, BELLE2-PUB-PH-2018-001, FERMILAB-PUB-18-398-T, JLAB-THY-18-2780, INT-PUB-18-047, UWThPh 2018-26 [arXiv:1808.10567].